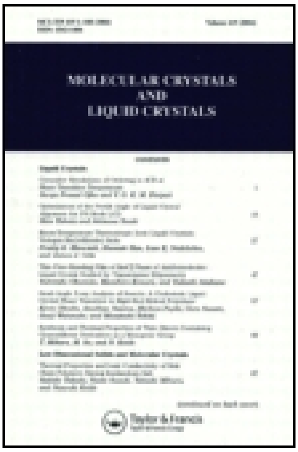

Molecular Crystals and Liquid Crystals
Publication details, including instructions for authors and subscription information:
http://www.tandfonline.com/loi/gmcl20

Solitons in Quasi-One-Dimensional Binuclear Metal Complexes

Shoji Yamamoto [a]
[a] Department of Physics, Okayama University, Okayama, 700-8530, Japan

Version of record first published: 18 Oct 2010

To cite this article: Shoji Yamamoto (2003): Solitons in Quasi-One-Dimensional Binuclear Metal Complexes, Molecular Crystals and Liquid Crystals, 379:1, 555-560

To link to this article: http://dx.doi.org/10.1080/713738611

Mol. Cryst. Liq. Cryst., Vol. 379, pp. 555-560

1058-725X/02 $12.00 + .00
DOI: 10.1080/10587250290091047

Solitons in Quasi-One-Dimensional Binuclear Metal Complexes

SHOJI YAMAMOTO

Department of Physics, Okayama University, Okayama 700-8530, Japan

We investigate soliton excitations in halogen (X)-bridged binuclear transition-metal (M) complexes (MMX chains), which are essentially characterized by competing intrasite and intersite electron-lattice couplings. Employing a simple electron-phonon model, their spatial and energy structures are calculated for two distinct ground states of MMX chains. In the weak-coupling region, all the solitons are degenerate and have close analogy with those in *trans*-polyacetylene.

Keywords: MMX chain; soliton; scaling properties

Recent intriguing observations [1,2] for halogen (X)-bridged binuclear transition-metal (M) linear-chain complexes (MMX chains) [3-5] have stimulated us to further explorations into the MX family compounds. MMX chains exhibit a wider variety of electronic states than the conventional MX compounds. Quantum [6], thermal [2] and pressure-induced [7,8] phase transitions between them have been activating not only theoretical calculations [9-12] but also materials research [13]. In such circumstances, the optical conductivity of MMX chains has recently been calculated [14], encouraging photoexperiments on these materials. Then we take interest in soliton excitations in this system and make the first step in this article.

We introduce a one-dimensional $\frac{3}{4}$-filled electron-phonon model:

$$\begin{aligned}\mathcal{H} = \frac{K_{\mathrm{MX}}}{2}\sum_n\Big[(u_n-v_n)^2+(v_n-u_{n-1})^2\Big] - t_{\mathrm{MM}}\sum_{n,s}(a_{n,s}^\dagger b_{n,s}+b_{n,s}^\dagger a_{n,s}) \\ -\sum_{n,s}\Big[t_{\mathrm{MXM}}-\alpha(v_{n+1}-v_n)\Big](b_{n,s}^\dagger a_{n+1,s}+a_{n+1,s}^\dagger b_{n,s}) \\ -\beta\sum_{n,s}\Big[(v_n-u_{n-1})a_{n,s}^\dagger a_{n,s}+(u_n-v_n)b_{n,s}^\dagger b_{n,s}\Big], \qquad (1)\end{aligned}$$

where $a_{n,s}^\dagger$ and $b_{n,s}^\dagger$ are the creation operators of an electron with spin s for the $\boldsymbol{M}\boldsymbol{d}_{z^2}$ orbitals in the nth MMX unit. α and β are the intersite and intrasite electron-phonon coupling constants, respectively. u_n and v_n are, respectively, the chain-direction displacements of the halogen and metal dimer in the nth MMX unit from their equilibrium position. The thus-far reported experimental observations suggest that every M_2 moiety is not deformed. We set t_{MM} and K both equal to unity.

This Hamiltonian possesses two distinct ground states and their competition is visualized in Figure 1. The CDW state is characterized by the alternating on-site energies, whereas the ACP state comparatively by the alternating interdimer transfer energies. The orbital hybridization within every M_2 moiety is essential in the valence-trapped CDW state, while it is the overlap of the d_{σ^*} orbitals on neighboring M_2 moieties that stabilizes the valence-delocalized ACP state. Therefore, increasing β and t_{MM} advantageously act on the CDW state, whereas increasing α and t_{MXM} on the ACP state. The calculations are well consistent with the experimental observations; $(NH_4)_4[Pt_2(pop)_4Cl]$ (pop = diphosphonate = $P_2O_5H_2^{2-}$) exhibits a ground state of the CDW type [15], while $Pt_2(dta)_4I$ (dta = dithioacetate = $CH_3CS_2^-$) displays that of the ACP type [2]. The M_2 moieties are tightly locked together in the pop complexes due to the hydrogen bonds between the ligands and the counter cations, whereas they are much more movable in the dta complexes owing to their neutral chain structure. Thus, considering that α indirectly describes the mobility of the M_2 sublattice, a significantly larger α is expected for $Pt_2(dta)_4I$.

Now we search for soliton solutions of the Hamiltonian (1). Under the constraint of the total chain length being unchanged, a trial wave function may be given as [16]

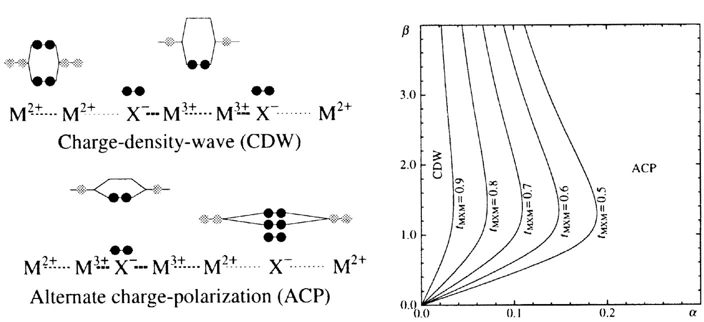

FIGURE 1. Schematic representation of the two distinct ground states of MMX chains and their ground state competition.

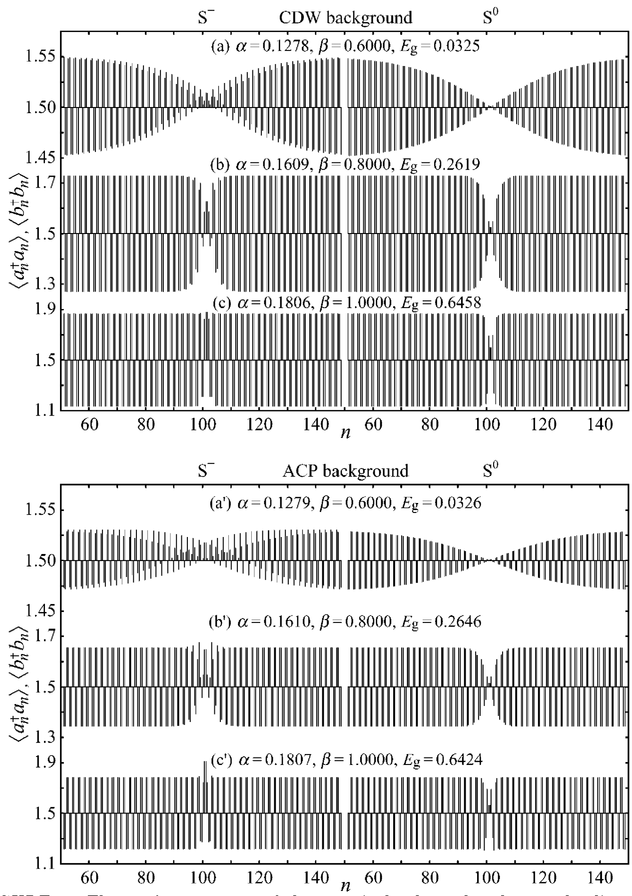

FIGURE 2. Electronic structures of the negatively charged and neutral solitons in the CDW (a,b,c) and ACP (a′,b′,c′) states.

$$u_n - v_n = \sigma(v_{n+1} - u_n) = (-1)^n l_0 \tanh\left[(na - x_0)/\xi_s\right], \qquad (2)$$

where σ takes $-$ and $+$ for the CDW and ACP backgrounds, respectively, a is the lattice constant, l_0 is the metal-halogen bond-length change in the ground state, and x_0 and ξ_s are, respectively, the soliton center and width, both of which are variationally determined. All the solitons are degenerate in the weak-coupling region but the degeneracy may be lifted in the strong-coupling region. The positively and negatively charged solitons ($S^{\pm}$) are not primarily degenerate due to no electron-hole symmetry, whereas the neutral solitons with up and down spins (S^0) are essentially degenerate because of the spin-rotational symmetry. When we compare the solitons in the CDW and ACP backgrounds, we calculate them in the vicinity of the phase boundary so as to illuminate their essential differences, if any. Taking the structural analyses [3,5] into consideration, we set $t_{\rm MM} = 2t_{\rm MXM}$.

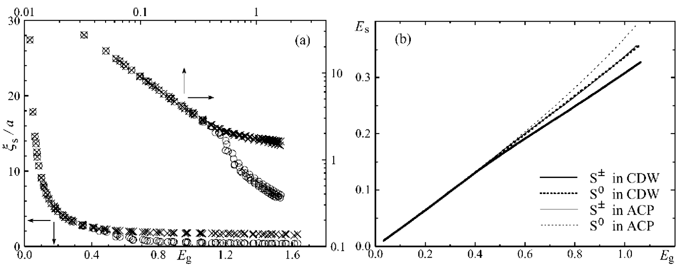

FIGURE 3. (a) The optimized width of the negatively charged soliton as a function of the band gap E_g in linear and logarithmic scales under various parametrizations, where $\circ$ and $\times$ correspond to the lowest- and highest-energy locations x_0, respectively. (b) The soliton formation energies E_s as functions of the band gap E_g, where E_s is averaged over x_0. The negatively and positively charged solitons possess more and less than three-quarter-filled electron bands, respectively, and therefore their formation energies can not be defined in themselves. As for the charged solitons, E_s is further averaged over S^+ and S^-.

We show in Figure 2 typical spatial structures of the optimum soliton solutions. Their formation energies E_s do not depend on their locations in the weak-coupling region, but the degeneracy is lifted in the strong-coupling region. As the coupling strength increases, solitons generally possess increasing energies and end up with immobile defects. In order to illuminate their scaling properties, we plot in Figure 3(a) ξ_s as a function of the band gap E_g. Although we take α and β at random, ξ_s is uniquely scaled by E_g as far as E_g stays not so large. We obtain a scaling formula $\xi_s/a \simeq 0.96/E_g^{0.98}$ which fits all the solitons $S^{\pm}$ and S^0. It is quite convincing that such a scaling law breaks down as ξ_s approaches a, where the chain no more behaves as a continuum. Figure 3(b) shows that the soliton energies are also scaled by E_g in the weak coupling region, which reads as $E_s \simeq 0.32E_g$. In the weak-coupling region, the $\frac{3}{4}$-filled binuclear metal units can be described in terms of effectively half-filled electron bands with the Fermi velocity v_{F} being given by

$$\hbar v_{\mathrm{F}} = 2at_{\mathrm{eff}}\,; \quad t_{\mathrm{eff}} = \frac{t_{\mathrm{MM}}t_{\mathrm{MXM}}}{2\sqrt{t_{\mathrm{MM}}^2 + t_{\mathrm{MXM}}^2}}\,. \tag{3}$$

Then the present Hamiltonian turns out [17] equivalent to the Takayama-Lin-Liu-Maki (TLM) continuum model [18] for *trans*-polyacetylene. The TLM scaling relations

$$\xi_{\mathrm{s}} = 4at_{\mathrm{eff}}/E_{\mathrm{g}}\,, \quad E_{\mathrm{s}} = E_{\mathrm{g}}/\pi\,, \tag{4}$$

with $t_{\mathrm{MM}} = 2t_{\mathrm{MXM}}$ well interpret the numerical observations.

Finally we discuss the energy structures with Figure 4. The background four bands of the CDW state are, from the bottom to the top, largely made up of the bonding combination ϕ_+ of binuclear Pt^{2+}-Pt^{2+} units, that of Pt^{3+}-Pt^{3+} units, the antibonding combination ϕ_- of Pt^{2+}-Pt^{2+} units and that of Pt^{3+}-Pt^{3+} units, while the major components of the four bands of the ACP state are the ϕ_+ orbitals of interdimer Pt^{2+}-X^--Pt^{2+} units, the ϕ_- orbitals of Pt^{2+}-X^--Pt^{2+} units, the ϕ_+ orbitals of Pt^{3+}-X^--Pt^{3+} units and the ϕ_- orbitals of Pt^{3+}-X^--Pt^{3+} units. Thus, in-

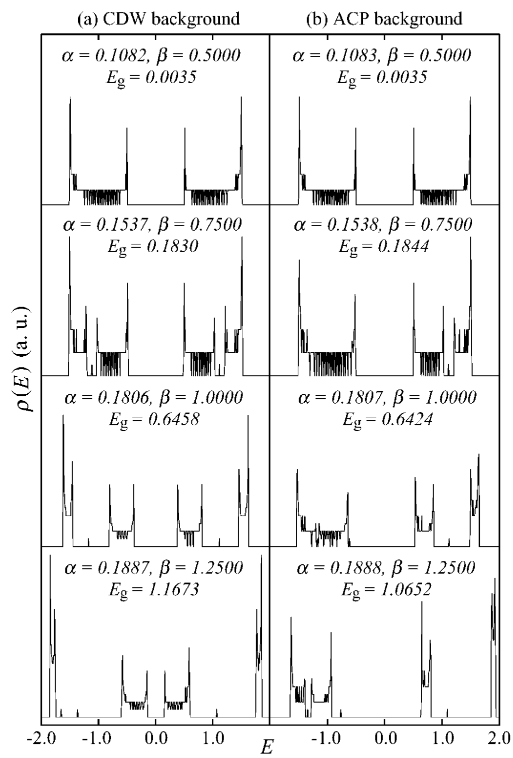

FIGURE 4. Density of states $\rho(E)$ for the optimum soliton solutions with the CDW (a) and ACP (b) backgrounds.

creasing β splits both σ and σ^* orbitals in the CDW state but relatively enhances the splitting between σ and σ^* orbitals in the ACP state. The optimum soliton solutions commonly exhibit an additional intragap level. In contrast with the case of polyacetylene [16], the soliton levels generally deviate from the middle of the gap in *MMX* chains. Since the tendency is more remarkable for the ACP background, the pop and dta complexes may be characterized from this point of view.

This work was supported by the Japanese Ministry of Education, Science and Culture and by the Sumitomo Foundation.

References

1) M. Yamashita, S. Miya, T. Kawashima, T. Manabe, T. Sonoyama, H. Kitagawa, T. Mitani, H. Okamoto and R. Ikeda, *J. Am. Chem. Soc.* **121**, 2321 (1999).
2) H. Kitagawa, N. Onodera, T. Sonoyama, M. Yamamoto, T. Fukawa, T. Mitani, M. Seto and Y. Maeda, *J. Am. Chem. Soc.* **121**, 10068 (1999).
3) C. Bellitto, A. Flamini, L. Gastaldi and L. Scaramuzza, *Inorg. Chem.* **22**, 444 (1983).
4) C. Bellitto, G. Dessy and V. Fares, *Inorg. Chem.* **24**, 2815 (1985).
5) C.-M. Che, F. H. Herbstein, W. P. Schaefer, R. E. Marsh and H. B. Gray, *J. Am. Chem. Soc.* **105**, 4604 (1983).
6) L. G. Butler, M. H. Zietlow, C.-M. Che, W. P. Schaefer, S. Sridhar, P. J. Grunthaner, B. I. Swanson, R. J. H. Clark and H. B. Gray, *J. Am. Chem. Soc.* **110**, 1155 (1988).
7) B. I. Swanson, M. A. Stroud, S. D. Conradson and M. H. Zietlow, *Solid State Commun.* **65**, 1405 (1988).
8) H. Matsuzaki and H. Okamoto, private communication.
9) M. Kuwabara and K. Yonemitsu: *J. Phys. Chem. Solids.* **62** (2001) 435.
10) S. Yamamoto, *Phys. Rev. B* **63**, 125124 (2001).
11) S. Yamamoto, *J. Phys. Soc. Jpn.* **70**, 1198 (2001).
12) S. Yamamoto, *Phys. Rev. B* **64**, 140102(R) (2001).
13) K. Sakai, Y. Tanaka, Y. Tsuchiya, K. Hirata, T. Tsubomura, S. Iijima and A. Bhattacharjee: *J. Am. Chem. Soc.* **120** (1998) 8366.
14) M. Kuwabara and K. Yonemitsu, *J. Mater. Chem.* **11**, 2163 (2001).
15) N. Kimura, H. Ohki, R. Ikeda, M. Yamashita, *Chem. Phys. Lett.* **220**, 40 (1994).
16) W. P. Su, J. R. Schrieffer and A. J. Heeger: *Phys. Rev. Lett.* **42**, 1698 (1979).
17) Y. Onodera: *J. Phys. Soc. Jpn.* **56**, 250 (1987).
18) H. Takayama, Y. R. Lin-Liu and K. Maki: *Phys. Rev. B* **21**, 2388 (1980).